User-centric Handover in mmWave Cell-Free Massive MIMO with User Mobility

Carmen D'Andrea, Giovanni Interdonato and Stefano Buzzi

Dipartimento di Ingegneria Elettrica e dell'Informazione, University of Cassino and Southern Latium, Cassino, Italy

{carmen.dandrea, giovanni.interdonato, buzzi}@unicas.it

Abstract—The coupling between cell-free massive multiple-input multiple-output (MIMO) systems operating at millimeter-wave (mmWave) carrier frequencies and user mobility is considered in this paper. First of all, a mmWave channel is introduced taking into account the user mobility and the impact of the channel aging. Then, three beamforming techniques are proposed in the considered scenario, along with a dynamic user association technique (handover): starting from a user-centric association between each mobile device and a cluster of access points (APs), a rule for updating the APs cluster is formulated and analyzed. Numerical results reveal that the proposed beamforming and user association techniques are effective in the considered scenario.

Index Terms—cell-free massive MIMO, millimeter-wave, user mobility, channel aging, handovers

I. INTRODUCTION

Cell-free massive MIMO is deemed a key technology for *beyond*-5G systems [1]–[3] mainly for its great ability to provide a uniformly excellent spectral efficiency (SE) throughout the network and ubiquitous coverage [4], [5]. Decentralizing operations such as channel estimation, power control and, possibly, precoding/combining prevents to create any bottleneck in the system, while confining the signal co-processing within a handful of properly, dynamically selected APs, implementing thereby a user-centric system [6], makes cell-free massive MIMO practical. Erasing the cell boundaries when transmitting/receiving data requires, however, smooth coordination and accurate synchronization among the APs.

The SE improvements that cell-free massive MIMO can provide over co-located massive MIMO and small cells are significant in the sub-6 GHz frequency bands, especially in terms of service fairness. In the mmWave bands, where achieving high spectral efficiency is not a concern thanks to the large available bandwidth, the distributed cell-free operation can certainly better cope with the hostile propagation environment at such high frequencies compared to a co-located system, as the presence of many serving APs in the user equipment (UE)'s proximity enhances coverage and link reliability. A few recent works have investigated the potential marriage between cell-free massive MIMO and mmWave under various viewpoints: energy efficiency maximization [7], analysis

in case of capacity-constrained fronthaul links [8], energy-efficient strategies to cope with a non-uniform spatial traffic distribution [9].

An aspect that deserves a closer look in this context is the impact on the performance of the UE mobility. As the UE moves, the propagation channels towards the APs are subject to time variations, and thereby the available channel state information (CSI) at the AP ages with time, effect called *channel aging*. The channel aging effects have been extensively analyzed for co-located massive MIMO [10], [11] (and references therein), and recently for cell-free massive MIMO [12] operating at sub-6 GHz frequency bands. While for mmWave bands, the effects of the channel aging have been evaluated for *Hetnet* MIMO systems in [13]. In most of the works in the literature, the channel aging is considered within a transmission block (or resource block) and usually intended as the mismatch between the acquired CSI prior the transmission, used for beamforming/combining, and the actual CSI at the transmission/reception time (channel estimation error aside).

Contributions: The novelty of this work consists in studying the coupling between cell-free massive MIMO, mmWave and user mobility. First of all, we introduce the mmWave channel model taking into account the user mobility and the impact of the channel aging. Then, we describe three beamforming techniques assuming different levels of complexity at the transmitter and receiver and propose a dynamic user association technique, which starts from a traditional user-centric approach and updates the serving cluster of APs for each user in order to reduce the number of unnecessary handovers. Numerical results reveal that the proposed beamforming and user association techniques are effective in the considered scenario.

II. SYSTEM MODEL

Let us consider a cell-free massive MIMO system operating at mmWave where M multi-antenna APs simultaneously serve K multi-antenna UE in the same time-frequency resources in time-division duplex (TDD) mode. We assume that both the APs and the UE are equipped with a uniform linear array (ULA) with random orientations, and steering angles taking on values in $[-\pi/2, \pi/2]$. Each AP and each UE has N_{AP} and N_{UE} antenna elements, respectively, with $MN_{\mathsf{AP}} > KN_{\mathsf{UE}}$. Finally, let $n_{\mathsf{s}} < \min(N_{\mathsf{AP}}, N_{\mathsf{UE}})$ be the number of streams multiplexed over the MIMO channel.

Unlike most of the works in the literature, we consider a channel that (almost) continuously evolves over time according to the variation of the UE locations with respect to the APs, hence according to a model that takes into account the UE mobility.

A. Channel Model

1) mmWave MIMO Channel Representation: The mmWave MIMO narrow-band channel between UE k and AP m consists in a dominant line-of-sight (LoS) path and $L_{km} \ll \min(N_{AP}, N_{UE})$ non-LoS (NLoS) paths due to the presence of scattering clusters. At the time instant n, $n = \{1, 2, 3 \ldots\}$, the channel is modelled by the complex-valued $(N_{AP} \times N_{UE})$-dimensional matrix

$$\mathbf{H}_{mk}[n] = \varsigma \sum_{\ell=1}^{L_{mk}} \alpha_{mk}^{(\ell)}[n] \mathbf{a}_{AP}(\phi_{mk}^{(\ell)}[n]) \mathbf{a}_{UE}^{H}(\theta_{mk}^{(\ell)}[n]) + \mathbf{H}_{mk}^{LoS}[n],$$
(1)

where $\varsigma = \sqrt{N_{AP} N_{UE}}$ is a normalization factor, $\alpha_{mk}^{(\ell)}[n] \sim \mathcal{CN}(0, \beta_{mk}^{(\ell)}[n])$ is the complex-valued gain of the ℓ-th path with strength (which reflects the path loss) denoted by $\beta_{mk}^{(\ell)}[n]$. The unit-norm ULA steering vectors at UE k and AP m are denoted by $\mathbf{a}_{UE}(\theta_{mk}^{(\ell)}[n])$ and $\mathbf{a}_{AP}(\phi_{mk}^{(\ell)}[n])$, respectively, highlighting the dependency on the angle of departure (AoD), $\theta_{mk}^{(\ell)}[n]$, and the angle of arrival (AoA), $\phi_{mk}^{(\ell)}[n]$, of the ℓ-th path. Assuming half-wavelength spacing between the antenna elements of the ULA, the steering vectors for a generic AoD and AoA are given by

$$\mathbf{a}_{AP}(\phi) = \frac{1}{\sqrt{N_{AP}}}[1, e^{j\pi \sin \phi}, \ldots, e^{j\pi(N_{AP}-1)\sin \phi}]^{T}, \quad (2)$$

$$\mathbf{a}_{UE}(\theta) = \frac{1}{\sqrt{N_{UE}}}[1, e^{j\pi \sin \theta}, \ldots, e^{j\pi(N_{UE}-1)\sin \theta}]^{T}. \quad (3)$$

The LoS component of the channel matrix at the nth time instant, $\mathbf{H}_{mk}^{LoS}[n]$, is given by

$$\mathbf{H}_{mk}^{LoS}[n] = \varsigma \epsilon(d_{mk}^{LoS}[n]) \varrho_{mk}^{LoS}[n] \mathbf{a}_{AP}(\phi_{mk}^{LoS}[n]) \mathbf{a}_{UE}^{H}(\theta_{mk}^{LoS}[n]), \quad (4)$$

where

$$\varrho_{mk}^{LoS}[n] \triangleq \sqrt{\beta_{mk}^{LoS}[n]} e^{j\vartheta_{mk}[n]},$$

with $\vartheta_{mk}[n] \sim \mathcal{U}(0, 2\pi)$, and $\epsilon(d_{mk}^{LoS}[n]) \in \{0, 1\}$ denotes the binary blockage variable characterizing the LoS link between AP m and UE k with length $d_{mk}^{LoS}[n]$, and indicating whether the LoS path, at the nth time instant, is obstructed. The LoS channel strength is denoted by $\beta_{mk}^{LoS}[n] \gg \beta_{mk}^{(\ell)}[n], \ell = 1, \ldots, L_{mk}$.

2) User Mobility: UE mobility leads to temporal variations in the propagation environment resulting in a channel that ages with time. This channel aging is much more significant in mmWave systems than in sub-6 GHz systems as a time variation results in a larger phase variation at high frequency bands than at low frequency bands.

In this work, we assume a block-fading channel model wherein the path gains—the fast fading component of the channel—stay constant within a resource block of length τ_c channel uses (or time instants) and vary over the resource blocks. Whereas the ULA steering vectors and the channel variances stay constant over multiple resource blocks, for an interval with duration $\tau_s > \tau_c$ time instants. The temporal evolution of the NLoS path gains over the resource blocks is modeled through a first order autoregressive model [10], [11], such that a path gain at the current time instant $\alpha_{mk}^{(\ell)}[n]$, with $n = \{1, 2, 3 \ldots\}$, is a function of its previous state $\alpha_{mk}^{(\ell)}[n-1]$ and an innovation component $\widetilde{\alpha}_{mk}^{(\ell)}[n]$ as

$$\begin{cases} \delta_{mk}[n]\alpha_{mk}^{(\ell)}[n-1] + \bar{\delta}_{mk}[n]\widetilde{\alpha}_{mk}^{(\ell)}[n], & \text{if } n \bmod \tau_c = 1, \\ \alpha_{mk}^{(\ell)}[\lfloor n/\tau_c \rfloor], & \text{otherwise,} \end{cases} \quad (5)$$

with $\widetilde{\alpha}_{mk}^{(\ell)}[n] \sim \mathcal{CN}(0, \beta_{mk}^{(\ell)}[n])$ and independent of $\alpha_{mk}^{(\ell)}[n-1]$, $\lfloor \cdot \rfloor$ is the *floor* function, $\bar{\delta}_{mk}[n] = \sqrt{1 - \delta_{mk}^2[n]}$, and $\delta_{mk}[n]$ represents the temporal correlation coefficient of UE k with respect to AP m, which follows the Jake's model

$$\delta_{mk}[n] = J_0\left(2\pi f_{D,mk} nT\right), \quad (6)$$

with $J_0(\cdot)$ being the zeroth-order Bessel function of the first kind, and T being the sampling period. $f_{D,mk}$ is the maximum Doppler frequency between the k-th UE and the m-th AP given by $f_{D,mk} = \nu_{k,m} f_c / c$, where ν_{mk} is the radial velocity of UE k with respect to AP m in meters per second (m/s), $c = 3 \cdot 10^8$ m/s is the speed of light, and f_c is the carrier frequency in Hz.

Importantly, the temporal variation of the channel variances, both for LoS and NLoS, is modeled as

$$\beta_{mk}^{(\ell)}[n] = \begin{cases} f_{PL}(d_{mk}^{(\ell)}[n]), & \text{if } n \bmod \tau_s = 1, \\ \beta_{mk}^{(\ell)}[\lfloor n/\tau_s \rfloor], & \text{otherwise,} \end{cases} \quad (7)$$

namely the path loss is assumed to stay constant within τ_s channel uses. The function $f_{PL}(d_{mk}^{(\ell)}[n])$ denotes the path loss function which is characterized by the distance between the k-th UE and the m-th AP over the ℓ-th path at the n-th time instant, $d_{k,m}^{(\ell)}[n]$.

Similarly, the AoAs and the AoDs (both for LoS and NLoS) vary every τ_s channel uses, and their temporal evolution is modeled as in Eq. (8), shown at the top of the next page, where $f_G(\cdot)$ represents the geometric function depending on the propagation scenario. Whereas the phase shift of the LoS channel component, $\vartheta_{mk}[n]$, takes on a new random value uniformly distributed on the interval $[0, 2\pi]$ every resource block but stays constant within τ_c channel uses.

The variation of the k-th UE's location from the time instant n to $n + 1$ is modelled as

$$x_k[n+1] = x_k[n] + v_k T_s \cos \varphi_k, \quad (9)$$

$$y_k[n+1] = x_k[n] + v_k T_s \sin \varphi_k, \quad (10)$$

where $\varphi_k \in [0, 2\pi]$ is the direction of the movement and v_k is the speed of the k-th UE with respect to a reference system centred on the UE location and assuming that φ_k and v_k remain constant over τ_s channel uses. A new realization of the UE's location determines a new set of distances $\{d_{mk}^{(\ell)}\}$ and, as a consequence, a new set of coefficients $\{\beta_{mk}^{(\ell)}\}$.

$$\left(\phi_{mk}^{(\ell)}[n], \theta_{mk}^{(\ell)}[n]\right) = \begin{cases} f_{\mathsf{G}}(d_{mk}^{(\ell)}[n]), & \text{if } n \bmod \tau_{\mathsf{s}} = 1 \\ \left(\phi_{mk}^{(\ell)}[\lfloor n/\tau_{\mathsf{s}} \rfloor], \theta_{mk}^{(\ell)}[\lfloor n/\tau_{\mathsf{s}} \rfloor]\right), & \text{otherwise.} \end{cases} \tag{8}$$

B. Downlink Signal Model

Without loss of of generality, we assume $n_{\mathsf{s}} = 1$, i.e., only one stream is transmitted for each AP-UE pair. Let $\mathbf{u}_{mk}[n]$ be the N_{AP}-dimensional precoding vector between AP m and the UE k, and let $\mathbf{v}_k[n]$ be the N_{UE}-dimensional combining vector used at the k-th user. We also define $a_{mk}[n]$ as a binary parameter to indicate whether the m-th AP serves the k-th UE. More specifically,

$$a_{mk}[n] = \begin{cases} 1 & \text{if AP } m \text{ serves UE } k, \\ 0 & \text{otherwise.} \end{cases} \tag{11}$$

The downlink data signal sent by the m-th AP is given by the following N_{AP}-dimensional vector-valued waveform

$$\mathbf{s}_m[n] = \sum_{j=1}^{K} a_{mj}[n] \sqrt{\eta_{mj}[n]} \mathbf{u}_{mj}[n] x_{mj}[n], \tag{12}$$

where $x_{mj}[n]$ is the data symbol intended for the j-th UE, $\mathsf{E}\left\{|x_{mj}[n]|^2\right\} = 1, \forall j, m$, and $\eta_{mj}[n]$ is the transmit power. The signal received at the k-th UE after the combining operation can be then expressed as

$$\begin{aligned} r_k[n] = &\sum_{m=1}^{M} a_{mk}[n] \sqrt{\eta_{mk}[n]} \mathbf{v}_k^{\mathsf{H}}[n] \mathbf{H}_{mk}^{\mathsf{H}}[n] \mathbf{u}_{mk}[n] x_{mk}[n] \\ &+ \sum_{m=1}^{M} \sum_{j \neq k}^{K} a_{mj}[n] \sqrt{\eta_{mj}[n]} \mathbf{v}_k^{\mathsf{H}}[n] \mathbf{H}_{mk}^{\mathsf{H}}[n] \mathbf{u}_{mj}[n] x_{mj}[n] \\ &+ z_k[n], \end{aligned} \tag{13}$$

where $z_k[n] \sim \mathcal{CN}(0, \sigma_k^2[n])$ is additive noise.

Precoding and Combining: We analyze three beamforming techniques: long-term beamforming (LTB), short-term beamforming (STB) and analog beamforming (ABF). We consider two different implementations for both LTB and STB: (i) digital implementation (DI) and (ii) constant-modulus implementation (CI), which is also suitable for a hybrid (analog/digital) implementation. In the case of LTB, each AP and UE performs long-term precoding and long-term combining, respectively [14], which requires only the knowledge of the channel variances, AoAs and AoDs of the channel. We thereby define the ($N_{\mathsf{AP}} \times N_{\mathsf{AP}}$)-dimensional covariance matrix

$$\begin{aligned} \mathbf{R}_{mk}^{(\mathsf{AP})}[n] &= \mathsf{E}\left\{\mathbf{H}_{mk}[n]\mathbf{H}_{mk}^{\mathsf{H}}[n]\right\} \\ &= \varsigma^2 \epsilon(d_{mk}^{\mathsf{LoS}}[n]) \beta_{mk}^{\mathsf{LoS}}[n] \mathbf{a}_{\mathsf{AP}}(\phi_{mk}^{\mathsf{LoS}}[n]) \mathbf{a}_{\mathsf{AP}}^{\mathsf{H}}(\phi_{mk}^{\mathsf{LoS}}[n]) \\ &+ \varsigma^2 \sum_{\ell=1}^{L_{mk}} \beta_{mk}^{(\ell)}[n] \mathbf{a}_{\mathsf{AP}}(\phi_{mk}^{(\ell)}[n]) \mathbf{a}_{\mathsf{AP}}^{\mathsf{H}}(\phi_{mk}^{(\ell)}[n]), \end{aligned} \tag{14}$$
$$\tag{15}$$

and the ($N_{\mathsf{UE}} \times N_{\mathsf{UE}}$)-dimensional covariance matrix

$$\begin{aligned} \mathbf{R}_{mk}^{(\mathsf{UE})}[n] &= \mathsf{E}\left\{\mathbf{H}_{mk}^{\mathsf{H}}[n]\mathbf{H}_{mk}[n]\right\} \tag{16}\\ &= \varsigma^2 \epsilon(d_{mk}^{\mathsf{LoS}}[n]) \beta_{mk}^{\mathsf{LoS}}[n] \mathbf{a}_{\mathsf{UE}}(\theta_{mk}^{\mathsf{LoS}}[n]) \mathbf{a}_{\mathsf{UE}}^{\mathsf{H}}(\theta_{mk}^{\mathsf{LoS}}[n]) \\ &+ \varsigma^2 \sum_{\ell=1}^{L_{mk}} \beta_{mk}^{(\ell)}[n] \mathbf{a}_{\mathsf{UE}}(\theta_{mk}^{(\ell)}[n]) \mathbf{a}_{\mathsf{UE}}^{\mathsf{H}}(\theta_{mk}^{(\ell)}[n]). \tag{17} \end{aligned}$$

In the case of LTB-DI, the precoding vector $\mathbf{u}_{mk}^{(\mathsf{DI})}[n]$ is equal to the predominant eigenvector of the matrix $\mathbf{R}_{mk}^{(\mathsf{AP})}[n]$, while the combining vector $\mathbf{v}_k^{(\mathsf{DI})}[n]$ is equal to the predominant eigenvector of the matrix

$$\overline{\mathbf{R}}_k^{(\mathsf{UE})}[n] = \sum_{m=1}^{M} a_{mk}[n] \mathbf{R}_{mk}^{(\mathsf{UE})}[n]. \tag{18}$$

In the LTB-CI, the generic entry of the beamforming and combining vectors has constant modulus, and phase as that of its digital counterpart, i.e.,

$$\mathbf{u}_{mk}^{(\mathsf{CI})}[n] = \frac{1}{\sqrt{N_{\mathsf{AP}}}} e^{\mathsf{j}\angle \mathbf{u}_{mk}^{(\mathsf{DI})}[n]}, \quad \mathbf{v}_k^{(\mathsf{CI})}[n] = \frac{1}{\sqrt{N_{\mathsf{UE}}}} e^{\mathsf{j}\angle \mathbf{v}_k^{(\mathsf{DI})}[n]}. \tag{19}$$

where $\angle \cdot$ denotes the phase of the argument.

STB can be performed if and only if we ideally assume that both APs and UEs have knowledge of the instantaneous realization of the channel $\mathbf{H}_{mk}[n]$. In the case of STB-DI, the precoding vector is given by the predominant eigenvector of the matrix $\mathbf{H}_{mk}[n]\mathbf{H}_{mk}^{\mathsf{H}}[n]$, whereas the combining vector at the UE is given by the predominant eigenvector of the matrix defined as in (18) but with no expectation in (16). The expression of the STB-CI does not differ from that of LTB-CI, the precoding and combining vectors follow Eq. (19) with $\mathbf{u}_{mk}^{(\mathsf{DI})}[n]$ and $\mathbf{v}_k^{(\mathsf{DI})}[n]$ evaluated according to the STB-DI. Finally, the precoding and combining vectors for the ABF scheme are set as the steering vectors in (2) and (3) corresponding to the AoD and AoA of the strongest path, respectively, for each AP-UE pair.

III. USER ASSOCIATION TECHNIQUE

In order to detail the user association technique, we firstly define the *channel strength indicator* for the communication between the m-th AP and the k-th UE, denoted by $\rho_{mk}[n]$, which is equal to the predominant eigenvalue of the channel covariance matrix. Any UE is served by a *user-centric cluster* of APs, consisting of the N_{UC} APs with the largest channel strength indicator. We let $O_k^{(n)} : \{1, \dots, M\} \to \{1, \dots, M\}$ denote the operator sorting the AP indices by the descending order of the vector $[\rho_{1k}[n], \dots, \rho_{Mk}[n]]$, such that $O_k^{(n)}(1)$ gives the index of the AP with largest $\rho_{mk}[n]$. The set $\mathcal{M}_k[n]$ of the N_{UC} APs serving the k-th user is then given by

$$\mathcal{M}_k[n] = \{O_k^{(n)}(1), O_k^{(n)}(2), \dots, O_k^{(n)}(N_{\mathsf{UC}})\}. \tag{20}$$

Hence, if $m \in \mathcal{M}_k[n]$, then $a_{mk}[n] = 1$, and $a_{mk}[n] = 0$ otherwise. The evolution of the UE's location due to the mobility changes the relative channel strength indicators between APs and UEs and thus the UE-to-APs associations. In this paper, we propose the following UE-to-APs association finalized to reduce the number of instantaneous handovers which can negatively affect the system performance.

As we have assumed that the UE's mobility produces a non-negligible effect on the channel every τ_s samples, the UE-to-APs association updates accordingly, that is

$$\overline{\rho}_{mk}^{(q)} = \rho_{mk}\left[n : q = \lfloor n/\tau_s \rfloor\right]. \tag{21}$$

In order to reduce the number of instantaneous handovers, we define two *hysteresis parameters*: a value, ζ_{HO} say, and a control number, N_{HO} say, used to dynamically manage the user association. The proposed dynamic user association is summarized in Algorithm 1.

Algorithm 1 The proposed dynamic user association

1: Start with $q = 0$ and perform the initial user-centric approach based on the channel strength indicators $\overline{\rho}_{mk}^{(0)}$ and obtain the set $\mathcal{M}_k[0]$.
2: **for** $q = 1, 2, 3, \ldots$ **do**
3:   Evaluate the new $\overline{\rho}_{mk}^{(q)}$, $\forall m, k$;
4:   **for** $k = 1, \ldots, K$ **do**
5:     Define
$$m_k^-(q-1) = \arg \min_{m \in \mathcal{M}_k[q-1]} \overline{\rho}_{mk}^{(q-1)}$$
and
$$m_k^+(q) = \arg \max_{m \notin \mathcal{M}_k[q-1]} \overline{\rho}_{mk}^{(q)}.$$
6:     Replace the worst AP in $\mathcal{M}_k[q + N_{\mathsf{HO}}]$ *only if*
$$\frac{\overline{\rho}_{m_k^+(h+1)k}^{(h+1)} - \overline{\rho}_{m_k^-(h)k}^{(h)}}{\overline{\rho}_{m_k^-(h)k}^{(h)}} > \zeta_{\mathsf{HO}}, \tag{22}$$
with $h = q-1, q, q+1, \ldots, q+N_{\mathsf{HO}}-1$.
7:   **end for**
8: **end for**

The proposed dynamic user-association procedure is aimed at controlling and reducing the unnecessary handovers. Unnecessary handovers can be a consequence of temporary variations of the large scale fading coefficient caused by the user mobility. In order to reduce them, we consider the hysteresis parameters and change the set of the serving cluster of a generic user only if the condition in Eq. (22) is satisfied. The hysteresis condition in Eq. (22) controls, for a generic user in the system, that the AP that we are removing from the serving cluster is not temporarily in a blockage condition but the user is significantly moving away from it.

IV. NUMERICAL RESULTS

In our simulation setup, we assume an orthogonal frequency-division multiplexing (OFDM) system operating at

$f_0 = 28$ GHz with bandwidth $W = 500$ MHz. The subcarrier spacing is 480 kHz, and assuming that the length of the cyclic prefix is 7% of the OFDM symbol duration, i.e., $\tau_{\mathsf{CP}}\Delta_f = 0.07$, we obtain $t_0 = 2.23$ μs and $N_C = 1024$ subcarriers. The antenna heights are 10 m at the APs and 1.65 m at the UEs as in [6]. The additive thermal noise has a power spectral density of -174 dBm/Hz, while the front-end receiver at the APs and at the UEs has a noise figure of 9 dB. In order to avoid to exceed the simulation area due to mobility, the APs are uniformly distributed in a square area of 850 m $\times$ 850 m, while the initial position of the UEs are uniformly distributed in an inner centred square area of 350 m $\times$ 350 m. We set $K = 20$, $M = 120$, $N_{\mathsf{AP}} = 32$ and $N_{\mathsf{UE}} = 16$. We assume a number of total scatterers, $N_s = 200$, common to all the APs and UEs and uniformly distributed in the simulation area where the APs are located. To model the blockage, we assume that the communication between the m-th AP and the k-th UE takes place via the n-th scatterer, i.e., the n-th scatterer is one of the effective L_{mk} contributing to the channel in Eq. (1), if the rays between the m-th AP and the n-th scatterer and the k-th UE and the n-th scatterer *simultaneously* exist. We assume there exists a link between two entities, in our case one AP/UE and one scatterer, if they are in LoS, with a probability $P_{\mathsf{LoS}}(d)$ being function of the distance d between the two entities, and defined as [15], [16]

$$P_{\mathsf{LoS}}(d) = \min\left(20/d, 1\right)\left(1 - e^{-d/39}\right) + e^{-d/39}. \tag{23}$$

The function $f_{\mathsf{PL}}\left(d_{mk}^{(\ell)}[n]\right)$ follows the Urban Microcellular (UMi) Street-Canyon model in [15]. Note that, given the locations of scatterers, UEs and APs in the system, the corresponding AoAs, AoDs, path lengths and $f_{\mathsf{G}}(z)$ in Eq. (8) are obtained with straightforward geometric relationships. In the downlink data transmission phase, we assume equal power allocation, i.e., letting P_m^{dl} be the maximum transmit power at the m-th AP, we set $\eta_{mk}[n] = P_m^{\mathsf{dl}} / \sum_{j=1}^{K} a_{mj}$.

We evaluate the system performance by assuming that both the APs and the UEs perfectly know the channel variances, the AoAs and the AoDs whenever required.

The signal-to-interference-plus-noise ratio (SINR) at the n-th time instant, in case of perfect channel state information knowledge, is denoted by $\mathrm{SINR}_k[n]$ and from Eq. (13) it is equal to

$$\frac{\left|\sum_{m=1}^{M} a_{mk}^{[n]} \sqrt{\eta_{mk}[n]}\mathbf{v}_k[n]^{\mathsf{H}}\mathbf{H}_{mk}^{\mathsf{H}}[n]\mathbf{u}_{mk}[n]\right|^2}{\sum_{j \neq k}^{K} \left|\sum_{m=1}^{M} a_{mj}[n]\sqrt{\eta_{mj}[n]}\mathbf{v}_k[n]^{\mathsf{H}}\mathbf{H}_{mk}^{\mathsf{H}}[n]\mathbf{u}_{mj}[n]\right|^2 + \sigma_k^2[n]}.$$
$$\tag{24}$$

Hence, a downlink achievable rate for the UE k is given by $\mathrm{R}_k[n] = W \log_2\left(1 + \mathrm{SINR}_k[n]\right)$.

In Fig. 1 we report the CDF of the downlink rate per user in the considered scenario using the beamforming techniques detailed in Section II-B, both for the case of no-moving users, i.e., $v = 0$ km/h, and slow-moving users with $v \in [5, 10]$
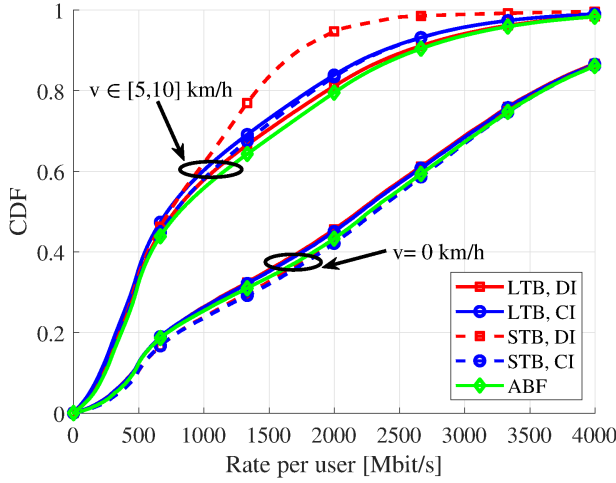
Fig. 1. CDF of downlink rate per user, comparison between the considered beamforming techniques in the cases of $v = 0$ km/h and $v \in [5, 10]$ km/h. Parameters: $N_{UC} = 5$, $\zeta_{HO} = 5$ % and $N_{HO} = 10$.

TABLE I
MEDIAN RATE (MR) AND 95%-LIKELY RATE (95-R) IN MBPS

UE speed	$v \in [5, 10]$ km/h				$v \in [20, 50]$ km/h			
Rate	MR		95-R		MR		95-R	
ζ_{HO}	5%	20%	5%	20%	5%	20%	5%	20%
LTB, DI	777	791	135	136	659	682	109	112
LTB, CI	720	734	122	123	617	638	102	105
STB, DI	736	749	149	151	648	669	122	126
STB, CI	776	791	146	148	649	684	123	127
ABF	814	830	156	158	684	709	129	133

km/h. For the proposed dynamic user association we assume that the hysteresis parameters are $\zeta_{HO} = 5$ % and $N_{HO} = 10$ and the dimension of the serving cluster for each user is $N_{UC} = 5$. Inspecting the results we can firstly note that the user mobility degrades the performance in terms of rate per user with respect to the case of no-moving users. Regarding the beamforming techniques, we can see that the LTB, which is more suitable for a practical implementation than the STB, offers good performance. We can also see that the ABF, which focuses the power only in the main AoA and AoD for each pair UE-AP is effective, especially in the case of user mobility. This behaviour is due to the sparse nature of the mmWave channel which allows us, on one hand, to focus the transmit power in few directions and, on the other hand, to reduce the interference in the system. Similar insights can be also obtained by the results in Table I which reports the median Rate (MR) and 95%-likely rate (95-R) of the system assuming the different beamforming techniques in the cases of slow-moving users with $v \in [5, 10]$ km/h and fast-moving users with $v \in [20, 50]$ km/h.

V. CONCLUSIONS AND FUTURE WORK

In this paper we considered a cell-free massive MIMO scenario at mmWave with UE mobility. First of all, we

introduced the channel model taking into account the user mobility and the impact of the channel aging and described three beamforming techniques assuming different levels of complexity. Taking into account the impact of the user mobility, we proposed a dynamic user association technique, which starts from a traditional user-centric approach and updates the serving cluster of APs for each user in order to reduce the number of unnecessary handovers. Numerical results reveal that the proposed techniques are effective and motivate us to deepen on this topic. In particular, the presented results assumed perfect knowledge of the channel variances, the AoAs and the AoDs and thus, further investigations are required on the impact of channel estimation error and the use of a protocol which exploits the sparse and autoregressive nature of the channel realizations.

REFERENCES

[1] J. Zhang, E. Björnson, M. Matthaiou, D. W. K. Ng, H. Yang, and D. J. Love, "Prospective multiple antenna technologies for beyond 5G," *IEEE J. Sel. Areas in Commun.*, vol. 38, no. 8, pp. 1637–1660, Aug. 2020.
[2] N. Rajatheva, I. Atzeni, E. Björnson, A. Bourdoux, S. Buzzi, J.-B. Dore, S. Erkucuk, M. Fuentes, K. Guan, Y. Hu *et al.*, "White paper on broadband connectivity in 6G," *arXiv preprint 2004.14247*, 2020.
[3] M. Matthaiou, O. Yurduseven, H. Q. Ngo, D. Morales-Jimenez, S. L. Cotton, and V. F. Fusco, "The road to 6G: Ten physical layer challenges for communications engineers," *IEEE Commun. Mag.*, vol. 59, no. 1, pp. 64–69, 2021.
[4] H. Q. Ngo, A. Ashikhmin, H. Yang, E. G. Larsson, and T. L. Marzetta, "Cell-free massive MIMO versus small cells," *IEEE Trans. Wireless Commun.*, vol. 16, no. 3, pp. 1834–1850, Mar. 2017.
[5] G. Interdonato, E. Björnson, H. Q. Ngo, P. Frenger, and E. G. Larsson, "Ubiquitous cell-free massive MIMO communications," *EURASIP J. Wireless Commun. and Netw.*, vol. 2019, no. 1, p. 197, 2019.
[6] S. Buzzi, C. D'Andrea, A. Zappone, and C. D'Elia, "User-centric 5G cellular networks: Resource allocation and comparison with the cell-free massive MIMO approach," *IEEE Trans. Wireless Commun.*, vol. 19, no. 2, pp. 1250–1264, Feb. 2020.
[7] M. Alonzo, S. Buzzi, A. Zappone, and C. D'Elia, "Energy-efficient power control in cell-free and user-centric massive MIMO at millimeter wave," *IEEE Trans. Green Commun. and Netw.*, vol. 3, no. 3, pp. 651–663, Sep. 2019.
[8] G. Femenias and F. Riera-Palou, "Cell-free millimeter-wave massive MIMO systems with limited fronthaul capacity," *IEEE Access*, vol. 7, pp. 44 596–44 612, Apr. 2019.
[9] J. García-Morales, G. Femenias, and F. Riera-Palou, "Energy-efficient access-point sleep-mode techniques for cell-free mmWave massive MIMO networks with non-uniform spatial traffic density," *IEEE Access*, vol. 8, pp. 137 587–137 605, Jul. 2020.
[10] K. T. Truong and R. W. Heath, "Effects of channel aging in massive MIMO systems," *Journal of Communications and Networks*, vol. 15, no. 4, pp. 338–351, Sep. 2013.
[11] A. K. Papazafeiropoulos, "Impact of general channel aging conditions on the downlink performance of massive MIMO," *IEEE Trans. Veh. Technol.*, vol. 66, no. 2, pp. 1428–1442, Feb. 2017.
[12] J. Zheng, J. Zhang, E. Björnson, and B. Ai, "Cell-free massive MIMO with channel aging and pilot contamination," in *Proc. of IEEE Global Commun. Conf. (GLOBECOM)*, Dec. 2020, pp. 1–6.
[13] A. Papazafeiropoulos, "Impact of hardware impairments and channel aging in millimeter-wave heterogeneous networks," in *Proc. of IEEE Wireless Commun. and Netw. Conf. (WCNC)*, Apr. 2019, pp. 1–7.
[14] M. R. Akdeniz, Y. Liu, M. K. Samimi, S. Sun, S. Rangan, T. S. Rappaport, and E. Erkip, "Millimeter wave channel modeling and cellular capacity evaluation," *IEEE J. Sel. Areas Commun.*, vol. 32, no. 6, pp. 1164–1179, Jun. 2014.
[15] A. Ghosh *et al.*, "5G channel model for bands up to 100 GHz," *5GCM white paper*, Oct. 2016.
[16] K. Haneda *et al.*, "5G 3GPP-like channel models for outdoor urban microcellular and macrocellular environments," in *Proc. of IEEE Veh. Technol. Conf. (VTC Spring)*, May 2016, pp. 1–7.